Twist1-Mediated Adriamycin-Induced Epithelial-Mesenchymal Transition Relates to Multidrug Resistance and Invasive Potential in Breast Cancer Cells

Qing-Quan Li,[1] Jing-Da Xu,[1] Wen-Juan Wang,[1] Xi-Xi Cao,[1] Qi Chen,[1] Feng Tang,[2] Zhong-Qing Chen,[2] Xiu-Ping Liu,[1] and Zu-De Xu[2]

Abstract

Purpose: Besides its therapeutic effects, chemotherapeutic agents also enhance the malignancy of treated cancers in clinical situations. Recently, epithelial-mesenchymal transition (EMT) has attracted attention in studies of tumor progression. We aimed to test whether transient Adriamycin treatment induces EMT and apoptosis simultaneously in cancer cells, clarify why the same type of cells responds differentially (i.e., apoptosis, EMT) to Adriamycin treatment, and elucidate the role of Twist1, the master regulator of EMT, in this process.

Experimental Design: In unsynchronized MCF7 cells or cells synchronized at different phases, apoptosis, EMT, and concurrent events [multidrug resistance (MDR) and tumor invasion] after Adriamycin or/and Twist1 small interfering RNA treatment were examined *in vitro* and *in vivo*. The Adriamycin-induced Twist1 expression and the interaction of Twist1 with p53-Mdm2 were examined by immunoblotting and immunoprecipitation, respectively.

Results: We showed *in vitro* that Adriamycin induced EMT and apoptosis simultaneously in a cell cycle–dependent manner. Only the cells undergoing EMT displayed enhanced invasion and MDR. Twist1 depletion completely blocked the mesenchymal transformation, partially reversed MDR, and greatly abolished invasion induced by Adriamycin. Also, we confirmed *in vivo* that Twist1 RNA interference improved the efficacy of Adriamycin for breast cancers. Further, Twist1 reduction in Adriamycin-treated cells promoted p53-dependent p21 induction and disrupted the association of p53 with Mdm2.

Conclusions: Our studies show the diverse responses to Adriamycin treatment in cells at different phases, suggest an unrecognized role of EMT in regulating MDR and invasion, and show the efficacy of Twist1 RNA interference in Adriamycin-based chemotherapies for breast cancer.

The resistance of tumor cells to multiple chemotherapeutic agents, a mechanism termed multidrug resistance (MDR), is a major obstacle to the success of cancer chemotherapy and has been closely associated with treatment failure (1). Previous research reported that transient exposure to chemotherapeutic drugs induces P-glycoprotein (P-gp) and *MDR1* mRNA expression in subpopulations of treated cancer cells, and the cells overexpressing P-gp display variations in invasive and metastatic behavior (2, 3). However, the detailed mechanism(s) underlying these phenomena still remains unclear.

The cellular transformations that modulate these capabilities seem analogous to some of the changes required for the acquisition of more aggressive phenotypes. Epithelial-mesenchymal transition (EMT), which disaggregates structured epithelial units to enable cell motility and morphogenesis in embryonic development, has attracted attention in studies of tumor progression (4–7). The most prominent characteristic of EMT is the morphologic alteration from epithelial to mesenchymal, which is often accompanied by the dissolution of epithelial tight junctions, loss of cell adhesion, down-regulated expression of some epithelial markers as well as the acquisition of migratory and invasive properties. Along with these changes, the cytoskeleton of the cells rearranges to render the cells with a spindle-like morphology (8). EMT is a complex process involving the genetic mutations that confer cancer developmental and malignant phenotypes and is critically linked with up-regulated invasion, metastasis, and angiogenesis (9, 10). The normal cellular processes involved in EMT during development are thought to play key roles in the multiphase evolution from a benign to an invasive malignant tumor (11).

The basic helix-loop-helix transcription factor Twist1 is a major regulator of mesenchymal phenotypes (12). It has also been recently identified as capable of mediating carcinoma

Authors' Affiliations: [1]Department of Pathology, Shanghai Medical College and [2]Department of Pathology, Huashan Hospital, Fudan University, Shanghai, China
Received 9/14/08; revised 12/4/08; accepted 12/4/08; published OnlineFirst 3/31/09.
Grant support: National Nature Science Foundation of China grants 30870972 and 30872971, Shanghai Board of Health grant 044082, and Funds of Shanghai Scientific Association grant 05ZR14023.
The costs of publication of this article were defrayed in part by the payment of page charges. This article must therefore be hereby marked *advertisement* in accordance with 18 U.S.C. Section 1734 solely to indicate this fact.
Note: Supplementary data for this article are available at Clinical Cancer Research Online (http://clincancerres.aacrjournals.org/).
Requests for reprints: Xiu-Ping Liu and Zu-De Xu, Department of Pathology, Shanghai Medical College, Fudan University, 138 Yi Xue Yuan Road, Shanghai 200032, China. Phone: 86-21-54237536; Fax: 86-21-54237596; E-mail: xpliu1228@fudan.edu.cn.

doi:10.1158/1078-0432.CCR-08-2372

Translational Relevance

Our study well explains the opposite effects of chemotherapy and provides the possible strategies in clinical oncotherapy as follows:

On one hand, because breast cancer cells at different phases respond differentially to Adriamycin treatment, it is essential to determine the cell cycle before the administration of chemotherapeutic agents in clinical situations. On the other hand, our data revealed that Twist1 is a multipotent molecule involved in the regulation of epithelial-mesenchymal transition, apoptosis, multidrug resistance, and tumor metastasis; the concomitant use of Twist1small interfering RNA during chemotherapy should be a potential therapeutic approach to improve the efficacy of Adriamycin for breast cancer.

In summary, this study provides further insight into the mechanism underlying the diverse cellular effects in response to Adriamycin treatment in breast cancer, pinpoints the inhibitive point that effectively down-regulates multidrug resistance and tumor invasion in a simultaneous manner, and enlightens the appropriate choice for therapeutic time in clinical practice.

metastasis. Endogenous Twist1 expression is found to be correlated with metastatic potential in a panel of human epithelial tumor cell lines (13–16). Twist1 inhibition through RNA interference (RNAi) is sufficient to greatly impair the metastatic ability of the most fully metastatic tumor cell line, 4T1 (14). Moreover, further studies also imply that Twist1 participates in regulating tumor resistance to paclitaxel in prostate cancer cells (17). We hypothesized that Twist1 expression may induce a significant change in the gene expression pattern of cancer cells and promote their acquisition of more aggressive phenotypes.

Here, we reported that Adriamycin induced apoptosis and EMT simultaneously in breast cancer cells depending on the phases of cell cycle. Only the cells undergoing EMT displayed up-regulation of P-gp, MDR to chemotherapeutic agents as well as increased *in vitro* invasive potentials. These acquired phenotypes were attenuated *in vitro* and *in vivo* by Twist1 RNAi, suggesting Twist1 as a promising therapeutic target against cancer in Adriamycin-based chemotherapy.

Materials and Methods

Cell culture and cell cycle synchronization. The human breast carcinoma cell line MCF7, the human colon adenocarcinoma DLD-1, and the human pancreatic cancer cells BxPC-3 were obtained from American Type Culture Collection and were maintained in RPMI 1640 containing 10% fetal bovine serum. The human hepatocellular carcinoma cell line HuH7 was provided by Professor Zhu HongGuang (Shanghai Medical College, Shanghai, China) and was maintained in Dulbecco's modified Eagle's medium supplemented with 10% fetal bovine serum. MCF7 cells were synchronized in G_1/S boundary by the addition of 2 mmol/L hydroxyurea (Sigma) to the medium for at least 16 h. G_2/M synchronization was achieved by maintaining the cells in culture with nocodazole (0.1 ng/mL; Sigma) for at least 20 h. After being synchronized to G_1/S or G_2/M phase, cells were treated with Adriamycin (25 μg/mL; Sigma) for another 36 h for EMT analysis or 72 h for apoptotic analysis in the presence of hydroxyurea or nocodazole.

Examination of morphologic change. The morphologic changes of the cells were observed under the inverted phase contrast microscope (Olympus). The photographs were taken with a Nikon digital camera (Nikon).

Flow cytometry assay. Flow cytometry was used to quantitatively detect the apoptotic rate. Cells (1×10^6) were plated into 10-cm tissue culture dishes 1 d before the treatment and were then treated with different types of external stresses. After the treatment, floating and attached cells were harvested, washed with PBS, fixed in 70% ethanol overnight at 4°C, and stained with 50 mg/mL propidium iodide (Sigma). The sub-G_1 peak (DNA content <2N) was measured with FACScan Flow Cytometry (Becton Dickinson Labware) and was analyzed by Cell Quest software.

Western blotting and co-immunoprecipitation. Total protein was extracted from cells with the use of RIPA lysis buffer (Santa Cruz Biotechnology). For Western blots, 50 μg of protein extract per lane were electrophoresed, transferred to polyvinylidene fluoride membranes, and incubated overnight with antibodies against E-cadherin (Santa Cruz Biotechnology, Inc.), CK19 (Santa Cruz), α-smooth muscle actin (SMA; Sigma), vimentin (Chemicon International), P-gp (Chemicon), Twist1 (Santa Cruz Biotechnology), p53 (Sigma), p21 (Sigma), and Mdm2 (Santa Cruz Biotechnology). The membranes were treated with the appropriate Alexa Fluor 700/800 nm–conjugated secondary antibodies (Invitrogen) and were analyzed with the use of the Odyssey Infrared Imaging System (Li-Cor BioSciences). For co-immunoprecipitation, 1 mg of protein lysate from each sample was incubated with 2 μg of anti-Twist1, p53, or Mdm2 overnight at 4°C. Then immunoblotting detections were done as described above.

Drug sensitivity assay. To assess their multidrug chemosensitivity, the cells under disposal and their corresponding controls were plated in 96-well plates at a density of 10^4 cells per well and further incubated for 24 h. The medium was then removed and replaced with fresh medium containing paclitaxel (Sigma), vincristine (Sigma), and bleomycin (Alexis Biochemicals) at varying concentrations for another 48 h. After that, cells were stained with 20 μL sterile 3-(4,5-dimethylthiazol-2-yl)-2,5-diphenyltetrazolium bromide dye at 37°C for 4 h followed by removal of culture medium and mixing of 150 μL DMSO thoroughly for 10 min. Spectrometric absorbance at 490 nm was measured with a microplate reader. Each group contained 3 wells and was repeated 3×. The half maximal inhibitory concentration value was determined by the dose of drug that causes 50% cell viability.

Tumor cell* in vitro *invasion assays. Transwell plates (Corning Costar) were coated with basement membrane Matrigel (0.8 mg/mL; Becton Dickinson) for 4 h at 37°C. The cells were detached with trypsin and washed with serum-containing medium. Cells (1×10^4) were added to the upper chamber in a total volume of 100 μL of serum-free medium supplemented with Adriamycin (25 μg/mL). The lower chamber contained 600 μL conditioned medium (incubating NIH3T3 cells in serum-free RPMI 1640 medium for 24 h) as chemoattractant. After 48 h, cells that migrated through the permeable membrane were fixed in methanol, stained with H&E, and counted. Each assay was done in triplicate and repeated 3×.

Inhibition of Twist1 expression by RNAi. To generate Adriamycin-induced Twist1-negative MCF7 cells, *Twist*-targeted RNAi experiments were done. Cells (2×10^5) were seeded in 6-well plates in triplicates and, after overnight incubation, the cells were transfected with various concentrations of small interfering RNA (siRNA) before Adriamycin treatment in serum-free Opti-MEM medium with the use of HiPerFect Reagent (Qiagen) as suggested by the manufacturer's instructions. After another 36 h of incubation with Adriamycin, total protein was extracted and gene expression was determined by western blotting. Anti–β-actin was used as protein loading control. The target sequence is *5-GGUACAUCGACUUCCUCUATT-3*, synthesized by Qiagen.

Twist1 siRNA–transfected cells invasion assay. Cells were tripsinized and resuspended in serum-free Opti-MEM (Gibco). From this single cell

suspension, 3×10^4 cells were seeded in the upper compartments that were then placed in the lower companion 24-well plate without cell culture medium. After 12 h of incubation, the cells were transfected with Twist1 siRNA, and the plate wells were filled with RPMI 1640 plus 10% fetal bovine serum without removing the upper compartments. After another 36 h of incubation with chemotherapeutic agents, a modified cell migration assay was done with the use of Matrigel Invasion Chambers as described above.

Twist1 transfection of MCF7 cells. The recombinant plasmid (named pCMV-Twist1) was a generous gift from Professor Masataka Nakamura (Tokyo Medical and Dental University, Tokyo, Japan). Transfection of MCF7 with pCMV-Twist1 was done with the use of Lipofectamine 2000 (Invitrogen) according to the manufacturer's instructions.

Murine xenograft model. Equal numbers (2×10^6) of MCF7 cells transfected with p*Silencer*-twist or p*Silencer* were harvested by trypsinization 2 d after transfection, washed twice with 1 × PBS, and resuspended in 0.2 mL of saline. Tumor xenografts were established by s.c. bilateral injection of the treated cells in log-phase growth into the flanks of athymic mice. When tumors measured an average volume of 80 mm^3, the mice (15 per group) were treated with Adriamycin (13.5 mg/kg; 3× weekly) or with 0.1 mL normal saline (pH 7.4; 3× weekly). The tumor size was measured by caliper twice weekly, and the tumor volume was calculated according to the following formula: V = (largest diameter × small diameter × depth) × π/6. At 35 d after inoculation, five mice in each group were sacrificed, and s.c. tumors were resected and fixed in 10% PBS. The remaining 10 mice in each group were maintained for observation of survival time and establishment of Kaplan-Meier survival curves. Animal experiments in this study were carried out in accordance with the institutional guidelines of Shanghai Medical College.

Statistical analysis. Statistics were calculated by SPSS software. The results are presented as mean ± SD (SE). ANOVA, Student's *t* test analysis, and Dunnett's multiple comparison tests were used to compare mean values. A *P* value of <0.05 was defined as statistically significant.

Results

Adriamycin induced EMT and apoptosis simultaneously in cancer cells. When the morphology of routinely cultured MCF7 cells treated with or without Adriamycin was examined by microscopy, we observed that, whereas MCF7 cells grew as tightly-packed colonies characteristic of epithelial cells and showed limited cell spreading, cells treated with Adriamycin seemed flattened and actively spreading, and had lost the majority of their cell-cell contacts (Fig. 1A). Similar effects were also observed in other epithelial cancer cells (HuH7, BxPC-3, and DLD-1; Supplementary Fig. S1A). These phenomena were associated with decreased expression of E-cadherin and CK19, and up-regulation of α-SMA, vimentin (Fig. 1B and Supplementary Fig. S1B). Because the loss of epithelial markers, including E-cadherin, cytokeratin, zonula occludens-1, and a corresponding increase in mesenchymal markers, such as vimentin, SMA, and/or fibroblast-specific protein 1, are the critical events signaling loss of the epithelial phenotype and commencement of mesenchymalization (5, 18–20), it can be concluded that Adriamycin induces EMT in epithelial cancer cells.

In our further studies, EMT induction was observed along with Adriamycin-induced cell damage. After incubation with Adriamycin for 72 hours, the percentage of cells undergoing apoptosis was significantly higher than that in the control group (Table 1 and Supplementary Fig. S1C). Moreover, drug-induced apoptosis was also detected by DNA fragmentation assays (Fig. 1C and Supplementary Fig. S1D).

Adriamycin treatment led to MDR in cancer cells, accompanied by enhanced invasive phenotype. Exposure of MCF7 cells to Adriamycin for 36 hours caused P-gp protein to become detectable by western blotting, and similar effects were

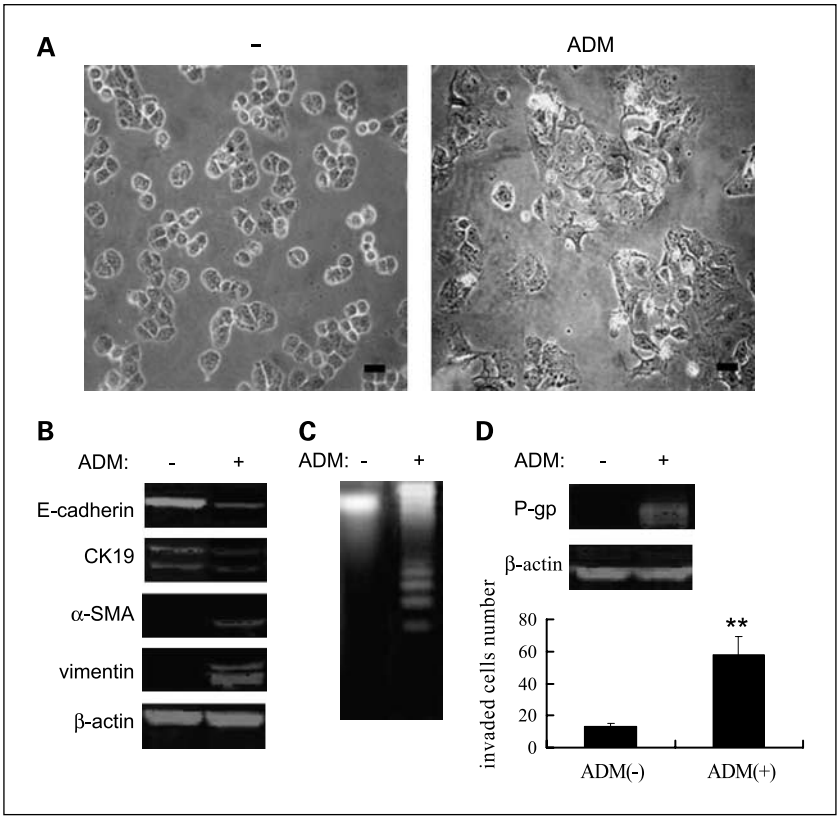

Fig. 1. Adriamycin induces apoptosis, EMT, and concurrent events in cancer cells. Cells were treated with or without Adriamycin (25 μg/mL) for 36 h for EMT analysis or 72 h for apoptotic analysis. *A,* EMT was examined by phase contrast photomicrographs (×100 magnification; bar, 10 μm). *B,* western blotting of E-cadherin, CK19, vimentin, and α-SMA was assessed. *C,* DNA was extracted and analyzed by 1.5% agarose gel electrophoresis. *D,* endogenous P-gp expression was measured by western blotting, and *in vitro* invasion assays were done. The number of invaded cells was evaluated in three fields for each experimental group and was averaged. Statistical analysis was done with Dunnett's test. **, $P < 0.05$ versus control cells.

Table 1. IC_{50} (paclitaxel, vincristine, bleomycin), apoptosis rate, and caspase activity in MCF7 cells at different phases; cells transfected with Twist siRNA or pCMV-Twist1; and cells pretreated with PFT-α after trasient Adriamycin exposure

	MCF7	Adriamycin-treated MCF7	Adriamycin-treated MCF7 synchronized at G_1/S phase	Adriamycin-treated MCF7 synchronized at G_2/M phase
Drugs				
Paclitaxel	0.0156 ± 0.0183	0.7562 ± 0.0238*	1.1365 ± 0.0421*	0.0103 ± 0.0056
Vincristine	0.3286 ± 0.0931	9.2321 ± 0.3561*	11.5638 ± 0.3397*	0.1867 ± 0.0048
Bleomycin	0.5644 ± 0.0339	4.8621 ± 0.3723*	5.2139 ± 0.2589*	0.3742 ± 0.0158
Apoptosis rate	0.0151 ± 0.0007	0.5239 ± 0.0143*	0.1419 ± 0.0051	0.8862 ± 0.0287*
Caspase activity (fold increase)				
Cas-1 (substrate IV)	1	2.3 ± 0.23*	1.21 ± 0.14	3.77 ± 0.34*
Cas-1 (substrate VII)	1	1.8 ± 0.05	1.27 ± 0.13	4.02 ± 0.39*
Cas-3	1	2.6 ± 0.21*	1.29 ± 0.11	6.38 ± 0.40*
Cas-6	1	2.9 ± 0.16*	1.20 ± 0.17	6.29 ± 0.33*
Cas-8	1	1.3 ± 0.09	1.34 ± 0.12	5.91 ± 0.38*

NOTE: IC_{50} values were expressed in μmol/L. Cell apoptosis rate was evaluated by flow cytometry. Caspase activity in nontreated cells was set as 1. Each assay was done in triplicate and repeated in triplicate, and all data were presented with mean ± SE. SDs for all of the experiments done in triplicate were <5%.
Abbreviations: IC_{50}, half maximal inhibitory concentration; dsRNA, double-stranded RNA; PFT-α, pifithrin-α.
*$P < 0.05$ versus control cells.

observed in other epithelial cancer cells (Fig. 1D and Supplementary Fig. S1E). Also, as reported in Table 1, Adriamycin-treated cells showed increased resistance to both P-gp substrates (vincristine, pacilitaxel) and a non–P-gp substrate (bleomycin). Thus, Adriamycin exposure led to a uniform decrease in drug sensitivity independent of whether the agents could be transported by P-gp.

The ability of Adriamycin-exposed MCF7 cells to invade through an artificial basement membrane (Matrigel) was assessed by *in vitro* invasion assay as described above. After

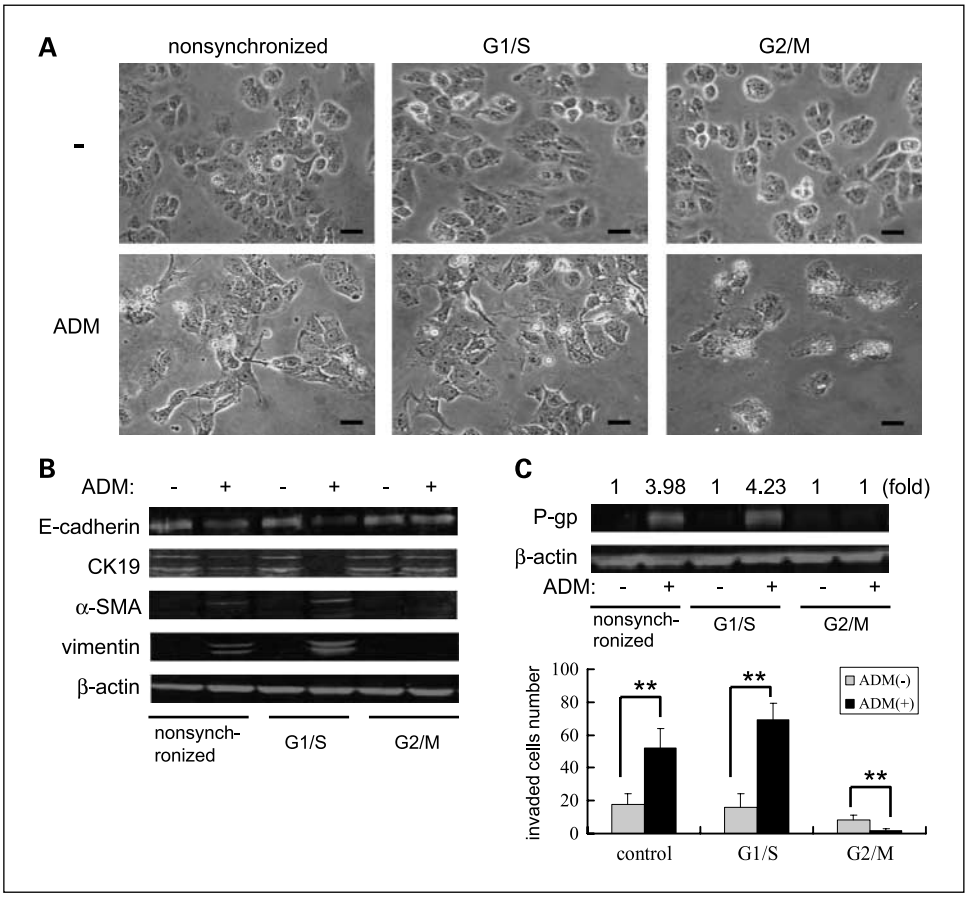

Fig. 2. Adriamycin-induced EMT and apoptosis are cell cycle dependent. Nonsynchronized cells and cells synchronized at G_1/S or G_2/M phase were treated with Adriamycin for the indicated times. *A,* EMT was examined by morphologic change (×200 magnification; bar, 10 μm). *B,* western blotting of E-cadherin, CK19, vimentin, and α-SMA was assessed. *C,* Adriamycin-induced P-gp expression and *in vitro* invasive potentials of synchronized cells in the presence or absence of Adriamycin were also determined. Quantification and statistical analyses were done on three independent experiments. **, $P < 0.05$ versus control cells.

Table 1. IC_{50} (paclitaxel, vincristine, bleomycin), apoptosis rate, and caspase activity in MCF7 cells at different phases; cells transfected with Twist siRNA or pCMV-Twist1; and cells pretreated with PFT-α after trasient Adriamycin exposure (Cont'd)

Adriamycin-treated dsRNA-transfected MCF7	Adriamycin-treated Twist1 siRNA–transfected MCF7	Adriamycin-treated pCMV-transfected MCF7	Adriamycin-treated pCMV-Twist1–transfected MCF7	PFT-α–pretreated MCF7	Adriamycin-treated PFT-α–pretreated MCF7
0.7964 ± 0.03581	*0.2492 ± 0.0351				
8.9637 ± 0.2886	*4.3688 ± 0.5294				
4.6630 ± 0.3051	*1.6197 ± 0.3513				
*0.4933 ± 0.0122	*0.8239 ± 0.0284	*0.5367 ± 0.018	0.0525 ± 0.009	0.0293 ± 0.0004	0.0622 ± 0.0003
*2.18 ± 0.25	*4.29 ± 0.36	*2.18 ± 0.25	1.23 ± 0.28	1.07 ± 0.08	1.04 ± 0.04
1.75 ± 0.14	*4.56 ± 0.38	1.75 ± 0.14	1.86 ± 0.17	1.15 ± 0.09	1.08 ± 0.15
*2.62 ± 0.27	*7.21 ± 0.45	*2.62 ± 0.27	1.55 ± 0.20	1.03 ± 0.10	1.05 ± 0.12
*2.98 ± 0.30	*6.98 ± 0.41	*2.98 ± 0.30	1.70 ± 0.26	1.00 ± 0.11	1.13 ± 0.07
1.30 ± 0.11	*5.44 ± 0.33	1.30 ± 0.11	1.25 ± 0.13	1.11 ± 0.06	1.09 ± 0.09

48 hours of culture, low numbers of MCF7 cells in the control group were observed to invade through the Matrigel. In contrast, when cultured in the presence of Adriamycin, the number of cells invading through the matrix was significantly greater (Fig. 1D); similar effects were also observed in other epithelial cancer cells (Supplementary Fig. S1E). In repeated invasion assays with different cancer cell lines, the invasiveness of the drug-exposed cells was found to be an average of 2.3-fold to 6.2-fold greater than that of the control group.

Adriamycin-induced apoptosis and EMT were cell cycle–dependent in breast cancer cells. Adriamycin induced concurrent but different events (EMT and apoptosis) in the same type of cells. To investigate the underlying mechanism, we examined the contribution of cell cycle state. We synchronized MCF7 cells at either G_1/S or G_2/M phase and examined Adriamycin-induced effects. As shown in Fig. 2A, Adriamycin induced morphologic changes in nonsynchronized cells and those synchronized at G_1/S phase, whereas it seemed to induce apoptosis in cells synchronized at G_2/M phase. To better characterize Adriamycin-induced EMT, we assessed the changes of tight junctions and cytoskeleton by immunofluorescent staining of zonula occludens-1 and β-actin, respectively.

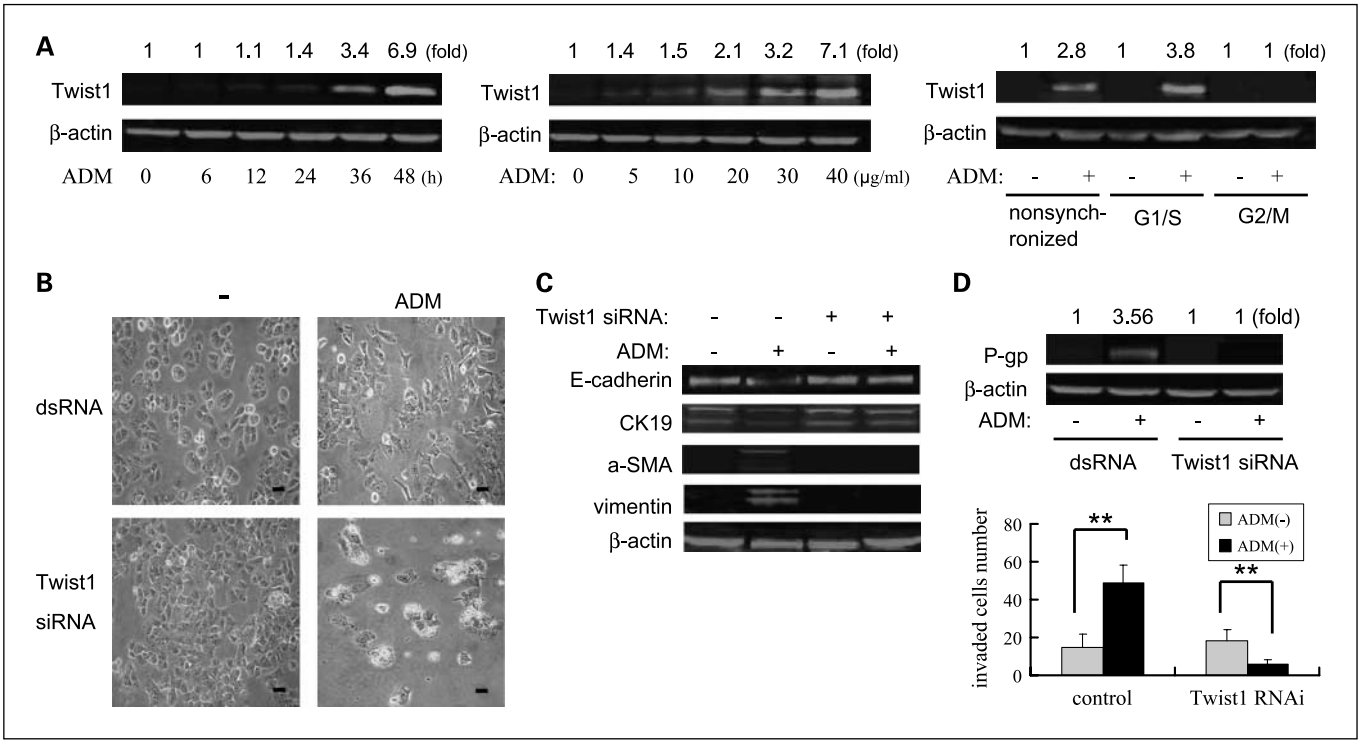

Fig. 3. Twist1 is involved in Adriamycin-induced EMT and concurrent events. *A,* time course and dose effect of Adriamycin-induced Twist1 expression in unsynchronized cell or cells synchronized at different phases. Cells transfected with control double-stranded RNA or Twist1 siRNA were treated with Adriamycin (25 μg/mL) for 36 h. EMT was examined by morphologic change (×100 magnification; bar, 10 μm) *B,* western blotting of E-cadherin, CK19, vimentin, and α-SMA was assessed (*C*). *D,* effects of Twist1 depletion on Adriamycin-induced P-gp expression and increased invasive potentials were determined by western blotting and *in vitro* invasion assays, respectively.
**, $P < 0.05$ versus control cells.

Supplementary Fig. S2 shows that Adriamycin induced the loss of tight junction and the rearrangement of cytoskeleton in nonsynchronized cells and cells at G_1/S phase but not in cells at G_2/M phase. Correspondingly, increased expression of α-SMA and vimentin, and down-regulation of E-cadherin and CK19 were also observed in nonsynchonized cells and cells at G_1/S phase (Fig. 2B). Meanwhile, Adriamycin tended to raise the apoptosis rate and caspase activity significantly only in cells at G_2/M phase (Table 1). These results clearly indicate that Adriamycin-induced apoptosis and EMT are related to the cell cycle state: apoptosis is induced mostly in cells at G_2/M phase, whereas EMT occurs only in cells at G_1/S phase.

Only cells undergoing EMT displayed MDR and elevated invasive abilities. As shown in Fig. 2C, Adriamycin induced P-gp expression in nonsynchronized MCF7 cells or those synchronized at G_1/S phase but not in cells at G_2/M phase. Corresponding results were observed in drug sensitivity assays (Table 1). Adriamycin also promoted *in vitro* invasion in nonsynchronized cells or those at G_1/S phase (Fig. 2C). The reduced number of invading cells synchronized at G_2/M phase could be mainly attributed to the drug-induced apoptosis.

Twist1 was identified as the key point in the process of Adriamycin-induced EMT and concurrent events. We next explored potential cellular events involved in Adriamycin-induced apoptosis and EMT. We found that Adriamycin induced Twist1 expression in both a time-dependent and a dose-dependent manner (Fig. 3A), whereas no similar effects were detected on other master regulators of EMT, such as Snail, Slug, and SIP1 (refs. 21–23; data not shown). Moreover, we observed that the appearance of Twist1 expression is ahead of morphologic changes. Additional experiments showed that Adriamycin-induced Twist1 expression could only be detected in cells at G_1/S but not G_2/M phase (Fig. 3A).

To test whether the up-regulation of Twist1 contributed to Adriamycin-induced responses, the effects of specific Twist1 siRNA on these events were evaluated. We used siRNA duplexes specific for human Twist1 as well as scrambled double-stranded RNA unrelated to any known gene as a control. The most effective concentration of siRNA tested (10 nmol/L) yielded a 92% Twist1 depletion (data not shown) and was used to examine the effects of Adriamycin on Twist1-negative cells. According to the changes in cell morphology (Fig. 3B) and the intracellular distribution of zonula occludens-1 and β-actin (Supplementary Fig. S3), Twist1 suppression blocked the drug-induced EMT, whereas the double-stranded RNA control showed no such effects. In line with these results, Twist1 siRNA reversed the effects of Adriamycin on E-cadherin, CK19, α-SMA, and vimentin expression (Fig. 3C). Also, we investigated whether Twist1 is involved in Adriamycin-induced apoptosis. Twist1 siRNA enhanced the apoptosis rate and caspase activity in response to Adriamycin treatment. On the contrary, this process was reversed by overexpression of Twist1 in Adriamycin-treated cells (Table 1).

Furthermore, Twist1 suppression prevented the drug-induced P-gp expression (Fig. 3D), concomitant with partial reduction in resistance to multiple agents (Table 1). This partial reduction in MDR implied that there may exist some other mechanism(s), in addition to Twist1, involved in Adriamycin-induced MDR. Twist1 siRNA also greatly decreased the invasive rate (Fig. 3D), which could be mainly ascribed to the elevated apoptosis rate.

Enhanced inhibition of tumor growth invasion and prolongation of survival in mice bearing breast tumors by combined pSilencer-twist and Adriamycin treatment. To improve and extend the results of *in vitro* experiments, we established a breast cancer model that mimics the clinical features. Tumor homogenates were subjected to western blot analysis for confirming Twist1 inhibition by pSilencer-twist treatment (data not shown). The antitumor effects of Adriamycin and pSilencer-twist were determined on MCF7 breast tumors. A significant growth inhibitory effect was observed in the treated groups as compared with the control groups. Indeed, after 35 days of treatment with Adriamycin in MCF7 and MCF7/pSilencer-twist tumors, the mean tumor volume was reduced by

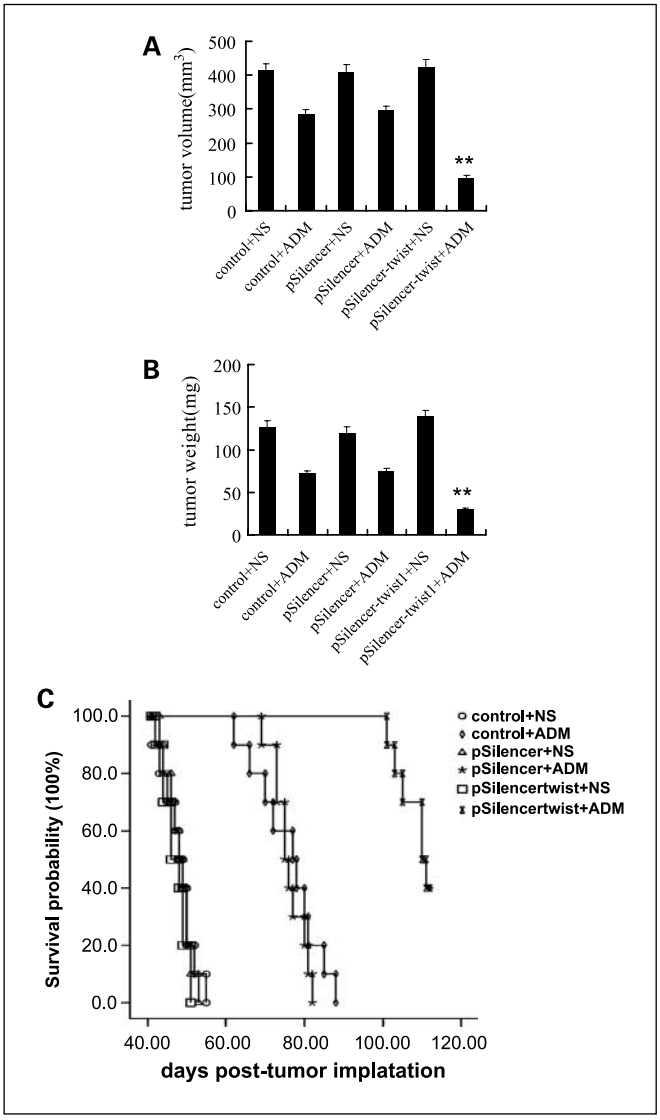

Fig. 4. Antitumor effects of Adriamycin are enhanced by pSilencer-twist. MCF7 cells transfected with pSilencer-twist or pSilencer were implanted s.c. When tumors reached an average volume of 80 mm^3, mice (15 per group) were treated with Adriamycin (13.5 mg/kg; 3× weekly) or 0.1 mL normal saline (pH 7.4, 3× weekly) for 35 d. Five mice were included in each group. Tumor volume (*A*) and weight (*B*) were measured at 35 d after inoculation with Adriamycin or saline. *C,* cumulative survival rate of nude mice implanted s.c. with MCF7 tumor cells. The survival curve was plotted according to the method of Kaplan-Meier ($n = 10$). **, $P < 0.05$ versus control cells.

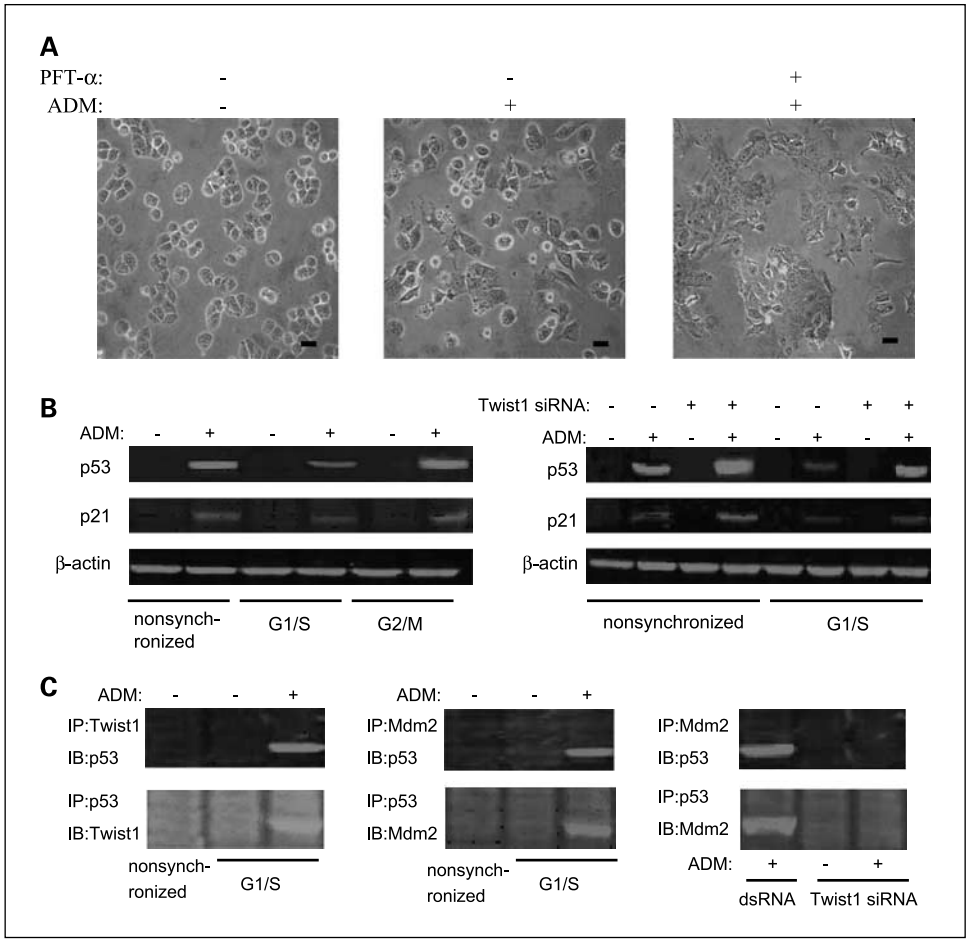

Fig. 5. Augmented interaction of Twist1 with p53 and Mdm2 in response to Adriamycin treatment dictates p53 response to chemotherapeutic agent. MCF7 cells pretreated with 20 μg/mL pifithrin-α were exposed to Adriamycin for the indicated times. *A,* EMT was examined by phase contrast photomicrographs (×100 magnification; bar, 10 μm). *B,* Adriamycin-induced expression of p53 and p21 in nonsynchronized cells and cells at G_1/S or G_2/M phase was determined by western blotting. MCF7 cells were transfected with Twist1 siRNA and treated with Adriamycin for 48 h. Subsequently, the lysates prepared from the treated cells were used for western blot analyses with the indicated antibodies. *C,* Twist1-depleted MCF7 cells were exposed to Adriamycin in the presence or absence of hydroxyurea for 48 h after treatment with a proteasome inhibitor (50 μmol/L; MG132) for 3 h; lysates prepared from the treated cells were immunoprecipitated with the indicated antibodies. The immunoprecipitates were then used for western blot analyses with the corresponding antibodies.

30.6% ($P > 0.05$) and 76.8% ($P < 0.05$; Fig. 4A), respectively, whereas the mean tumor weight was decreased by 42.4% ($P < 0.05$) and 78.2% ($P < 0.05$; Fig. 4B), respectively. At postmortem examination, no tumor metastasis was seen 35 days after s.c. injection of Adriamycin in MCF7/pSilencer-twist tumors, whereas pulmonary and lymphonodi metastasis foci could be found in control mice 20 days after receiving treatment of Adriamycin (data not shown). Seventeen weeks after treatment, the Kaplan-Meier plot assessment showed a significant prolongation of surviving mice bearing breast tumors after combined treatment (Adriamycin+pSilencer-twist). Figure 4C shows that the median survival time of untreated mice (PBS) was 48 days. In contrast, the median survival time of Adriamycin+pSilencer-twist–treated mice was significantly longer (110 days) than that of mice treated with Adriamycin or pSilencer-twist alone (77 and 48 days, respectively).

Twist1 dictated p53 response induced by Adriamycin via Mdm2 interaction. Adriamycin is a chemotherapeutic agent that is known to activate p53. After pretreatment with 20 μL/mL pifithrin-α (a small molecule inhibitor of p53 activity) for 4 hours, the apoptosis rate in Adriamycin-treated MCF7 cells was significantly lower (6.22%) than that in the control cells (52.39%), and so was the caspase activity (Table 1). Meanwhile, the number of cells undergoing EMT increased under the same condition (Fig. 5A), suggesting that Adriamycin induces apoptosis via a p53-dependent pathway in MCF7 cells. We also noted that after Adriamycin treatment, the induction of p53 and its target (p21) was markedly augmented in non-synchronized cells or those at G_2/M phase, whereas relatively less induction was noted in cells synchronized at G_1/S phase (Fig. 5B).

To examine the role of Twist1 in p53 activation, we introduced Twist1 siRNA into MCF7 cells and determined whether the reduced level of Twist1 affects the induction of p53 and p21 after Adriamycin exposure. In cells unsynchronized or synchronized at G_1/S phase, we observed that Twist1 reduction enhanced p53 and p21 production strikingly under the treatment of Adriamycin (Fig. 5B). In contrast, because Adriamycin did not induce Twist1 expression in cells at G_2/M phase, Twist1 siRNA had no such effects (data not shown).

The data presented above indicate that the expression level of Twist1 has significant effects on p53 and p21 induction. To obtain insight into the molecular mechanism of how such effects were achieved, we examined whether Adriamycin affects the physical interaction among p53, Mdm2, and Twist1. To avoid potential degradation of p53 via Mdm2-dependent ubiquitination, cells were treated with MG132, a proteasome inhibitor, before the interactions were examined by immunoprecipitation analyses. Figure 5C shows that the p53-Mdm2-Twist1 complex formed after Adriamycin exposure. Adriamycin treatment increased the association of p53 with Twist1 and Mdm2. On the other hand, Twist1 depletion decreased the formation of the p53-Mdm2 complex (Fig. 5C); from this

we inferred that Twist1 promotes the interaction of Mdm2 with p53.

Discussion

Chemotherapy is a systemic treatment involving the use of chemical agents to stop cancer cells from growing. Although chemotherapy effectively eliminates cancer cells, its opposite effects that enhance the malignancy of the treated cancers have also been reported (2, 24, 25). In a clinical situation, acquired drug resistance and enhanced metastasis frequently follow chemotherapeutic regimens, leading to treatment failure (i.e., cancer recurrence) in tumor patients. It seems that the syngeneic tumor cells may respond differently to the same chemotherapeutic drug. However, the detailed mechanism(s) underlying this phenomenon still remains unclear.

In the present study, we found that, except for Adriamycin-induced apoptosis, cancer cells exposed to Adriamycin transiently also showed EMT consistent with phenotypic changes, including MDR and enhanced invasive abilities. Adriamycin-induced EMT was first observed by morphologic changes, further validated by hallmarks of EMT. Recent publications implied that this is the case in chronic resistance to chemotherapeutic agents. Kajiyama et al. observed cellular morphology, motility, and molecular changes consistent with EMT in human stable paclitaxel-resistant epithelial ovarian carcinoma cells and suggested a possible link between chronic paclitaxel-resistance and EMT induction (26). Our results reflect the emergence of EMT after 36 hours of Adriamycin treatment. Therefore, it can be deduced that during the process of chemotherapy, EMT emerges at the very start. In view of the Adriamycin-induced concomitant EMT and apoptosis, a question was raised: why did Adriamycin induce the death of only a portion of cells but not all after a certain period of treatment? We hypothesized that, in response to Adriamycin treatment, some cells underwent the process of EMT and survived, thereby becoming the stable cell line resistant to chemotherapeutic agents at last.

Then another question arose: why, under the same experimental conditions, did the same type of cells respond differentially to Adriamycin treatment? The most likely factor that determines the various responses, and thus the different fates of cells, to the same stimuli should be differences that lie in the cells themselves. Because emerging evidence has shown that cell cycle state is an important factor for cellular responses to extracellular stimuli (27), we considered that there might be a relationship between cell cycle progression and Adriamycin-induced effects. We observed Adriamycin-induced EMT in both unsynchronized cells and those synchronized at G_1/S phase, whereas a dramatic increase was observed in the apoptosis rate of cells synchronized at G_2/M phase. These results indicated that Adriamycin-induced apoptosis and EMT are closely related with the cell cycle stage. We also showed that only cells undergoing EMT exhibited two malignant phenotypes, promoted invasion and MDR, which have been studied extensively and functionally linked with each other (28–32). The two phenotypes were coregulated and associated with EMT in cancers. In particular, in regular cell cultures without synchronization, cells are highly heterogeneous in terms of cell cycle phases and therefore respond differentially to Adriamycin, including apoptosis and EMT. For cells at G_1/S phase, Adriamycin promotes EMT and tumor progression characterized by acquisition of MDR and promoted invasive potential.

Our work also revealed that Twist1 may assume a dual role because it has intrinsic potential effects on EMT as well as an antiapoptotic function. On one hand, we found that Adriamycin induced Twist1 expression only in unsynchronized cells or cells synchronized at G_1/S phase, consistent with the emergence of EMT. Twist1 RNAi largely inhibited EMT induction, partially reversed MDR phenotype, and obviously abolished increased cell invasion of MCF7 cells. Combined Twist1 siRNA and Adriamycin treatment prevented tumor growth *in vivo* invasion and prolonged survival in mice bearing breast tumors. Consistent with its function in EMT, Twist1 was observed to be correlated with metastasis in various cancers, including ovarian, prostate, and nasopharyngeal cancers (33–36). Our data implicated that up-regulation of Twist1 seems to be a crucial event in EMT from low-grade to higher-grade malignant tumor cells. The concomitant use of Twist1 siRNA during chemotherapy can be a potential therapeutic approach to improve the efficacy of Adriamycin for breast cancer. Apart from these, because Twist1 is a master EMT regulator, it is reasonable to believe that acquisition of the malignant phenotypes after Adriamycin treatment is the byproduct during the process of EMT.

On the other hand, we found that Twist1 overexpression prevented cells from undergoing apoptosis in response to Adriamycin treatment. Twist1 has been reported to inhibit oncogene-dependent and *p53*-dependent cell death via inhibiting p14ARF expression or Mdm2 activity (37, 38). Adriamycin belongs to the DNA-damaging agent that provokes a p53 response (39). We first showed the formation of p53-Mdm2-Twist1 complex in Adriamycin-treated cells synchronized at G_1/S phase. The regulation of p53-Twist1 interaction by the external stimuli mainly reflected its effect on p53-Mdm2 interaction. Remarkably, the levels of the p53-Mdm2-Twist1 complex formed after Adriamycin treatment showed good correlation with the extent of Twist1-dependent inhibition of p21 activation under this condition. Therefore, it is likely that distinct effects of Adriamycin on p53 activation, at least in part, depend on how it impacts p53-Mdm2-Twist1 interaction. Because no Twist1 expression was observed in cells at G_2/M phase after Adriamycin treatment, MCF7 cells remained susceptible to the chemotherapeutic agent. Taken together with the data of flow cytometry, which showed that Twist1 RNAi raised the apoptosis rate of Adriamycin-treated MCF7 cells, we inferred that Twist1 depletion effectively enhances chemosensitivity to Adriamycin through disruption of the p53-Mdm2-Twist1 complex.

In summary, our data begin to clarify the mechanism involved in differential effects (i.e., apoptosis, EMT, and enhanced malignancy) in response to short-term Adriamycin treatment in cancers and also make evident the observed relationships between the differential effects and cell cycle state. It seems that suppression of the molecule associated with EMT, such as Twist1, could be an effective target for abolishing the opposite effects during clinical treatment of breast cancers in particular.

Disclosure of Potential Conflicts of Interest

No potential conflicts of interest were disclosed.

References

1. Kerbel RS. A cancer therapy resistant to resistance. Nature 1997;390:335–6.
2. Chaudhary PM, Roninson IB. Induction of multidrug resistance in human cells by transient exposure to different chemotherapeutic drugs. J Natl Cancer Inst 1993;85:632–9.
3. Yang JM, Xu Z, Wu H, Zhu H, Wu X, Hait WN. Overexpression of extracellular matrix metalloproteinase inducer in multidrug resistant cancer cells. Mol Cancer Res 2003;1:420–7.
4. Thiery JP. Epithelial-mesenchymal transitions in tumour progression. Nat Rev Cancer 2002;2:442–54.
5. Peinado H, Portillo F, Cano A. Transcriptional regulation of cadherins during development and carcinogenesis. Int J Dev Biol 2004;48:365–75.
6. Barrallo-Gimeno A, Nieto MA. The Snail genes as inducers of cell movement and survival: implications in development and cancer. Development 2005;132:3151–61.
7. Moody SE, Perez D, Pan TC, et al. The transcriptional repressor Snail promotes mammary tumor recurrence. Cancer Cell 2005;8:197–9.
8. Yang Y, Pan X, Lei W, et al. Regulation of transforming growth factor-β1-induced apoptosis and epithelial-to-mesenchymal transition by protein kinase A and signal transducers and activators of transcription 3. Cancer Res 2006;66:8617–24.
9. Yang J, Mani SA, Weinberg RA. Exploring a new Twist on tumor metastasis. Cancer Res 2006;66:4549–52.
10. Mironchik Y, Winnard PT, Jr., Vesuna F, et al. Twist overexpression induces *in vivo* angiogenesis and correlates with chromosomal instability in breast cancer. Cancer Res 2005;65:10801–9.
11. Huber MA, Kraut N, Beug H. Molecular requirements for epithelial-mesenchymal transition during tumor progression. Curr Opin Cell Biol 2005;17:1–11.
12. Kang Y, Massague J. Epithelial-mesenchymal transitions: Twist in development and metastasis. Cell 2004;118:277–9.
13. Hoek K, Rimm DL, Williams KR, et al. Expression profiling reveals novel pathways in the transformation of melanocytes to melanomas. Cancer Res 2004;64:5270–82.
14. Yang J, Mani SA, Donaher JL, et al. Twist, a master regulator of morphogenesis, plays an essential role in tumor metastasis. Cell 2004;117:927–39.
15. Kwok WK, Ling MT, Lee TW, et al. Up-regulation of TWIST in prostate cancer and its implication as a therapeutic target. Cancer Res 2005;65:5153–62.
16. Grunert S, Jechlinger M, Beug H. Diverse cellular and molecular mechanisms contribute to epithelial plasticity and metastasis. Nat Rev Mol Cell Biol 2003;4:657–65.
17. Wang X, Ling MT, Guan XY, et al. Identification of a novel function of TWIST, a bHLH protein, in the development of acquired Taxol resistance in human cancer cells. Oncogene 2004;23:474–82.
18. Okada H, Danoff TM, Kalluri R, et al. Early role of Fsp1 in epithelial-mesenchymal transformation. Am J Physiol 1997;273:563–74.
19. Lee JM, Dedhar S, Kalluri R, Thompson EW. The epithelial-mesenchymal transition: new insights in signaling, development, and disease. J Cell Biol 2006;172:973–81.
20. Thiery JP, Sleeman JP. Complex networks orchestrate epithelial-mesenchymal transitions. Nat Rev Mol Cell Biol 2006;7:131–42.
21. Cano A, Perez-Moreno MA, Rodrigo I, et al. The transcription factor snail controls epithelial-mesenchymal transitions by repressing E-cadherin expression. Nat Cell Biol 2000;2:76–83.
22. Comijn J, Berx G, Vermassen P, et al. The two-handed e box binding zinc finger protein sip1 down-regulates e-cadherin and induces invasion. Mol Cell 2001;7:1267–78.
23. Carver EA, Jiang R, Lan Y, Oram KF, Gridley T. The mouse snail gene encodes a key regulator of the epithelial-mesenchymal transition. Mol Cell Biol 2001;21:8184–8.
24. Yang JM, Medina GY, Vassil DJ, Liao AD, Hait J. Treatment of multidrug resistant (MDR1) murine leukemia with P-glycoprotein substrates accelerates the course of the disease. Biochem Biophys Res Commun 1999;266:167–73.
25. Yamauchi K, Yang M, Hayashi K, et al. Hoffman. Induction of cancer metastasis by cyclophosphamide pretreatment of host mice: an opposite effect of chemotherapy. Cancer Res 2008;68:516–20.
26. Kajiyama H, Shibata K, Terauchi M, et al. Chemoresistance to paclitaxel induces epithelial-mesenchymal transition and enhances metastatic potential for epithelial ovarian carcinoma cells. Int J Oncol 2007;31:277–83.
27. Sherr Charles J. Cancer cell cycles. Science 1996;274:1672–7.
28. Kerbel RS, Waghorne C, Korczak B, Lagarde A, Breitman ML. Clonal dominance of primary tumours by metastatic cells: genetic analysis and biological implications. Cancer Surv 1988;7:597–629.
29. Kerbel RS, Korczak B, Lagarde A. Growth dominance of the metastatic cancer cell: cellular and molecular aspects. Adv Cancer Res 1990;5:87–132.
30. Su ZZ, Austin VN, Zimmer SG, Fisher PB. Defining the critical gene expression changes associated with expression and suppression of the tumorigenic and metastatic phenotype in Ha-ras-transformed cloned rat embryo fibroblast cells. Oncogene 1993;8:1211–9.
31. Li QQ, Wang WJ, Xu ZD, et al. Involvement of CD147 in regulation of multidrug resistance to P-gp substrate drugs and *in vitro* invasion in breast cancer cells. Cancer Sci 2007;98:1064–9.
32. Li QQ, Wang WJ, Xu ZD, et al. Up-regulation of CD147 and matrix metalloproteinase-2, -9 induced by P-glycoprotein substrates in multidrug resistant breast cancer cells. Cancer Sci 2007;98:1767–74.
33. Leptin M, Grunewald B. Cell shape changes during gastrulation in Drosophila. Development 1990;110:73–84.
34. Hosono S, Kajiyama H, Terauchi M, et al. Expression of Twist increases the risk for recurrence and for poor survival in epithelial ovarian carcinoma patients. Br J Cancer 2007;96:314–20.
35. Kwok WK, Ling MT, Lee TW, et al. Up-regulation of Twist in prostate cancer and its implication as a therapeutic target. Cancer Res 2005;65:5153–62.
36. Song LB, Liao WT, Mai HQ, et al. The clinical significance of Twist expression in nasopharyngeal carcinoma. Cancer Lett 2006;242:258–65.
37. Maestro R, Dei Tos AP, Hamamori Y, et al. Twist is a potential oncogene that inhibits apoptosis. Genes Dev 1999;13:2207–17.
38. Okorokov AL, Orlova EV, Kingsbury SR, et al. Molecular structure of human Geminin. Nat Struct Mol Biol 2004;11:1021–2.
39. Saito S'i, Yamaguchi H, Higashimoto Y, et al. Phosphorylation site interdependence of human p53 post-translational modifications in response to stress. J Biol Chem 2003;278:37536–44.